

# Distinguishing the origin of the superconducting state from the pseudogap of high-temperature superconductors

E. V. L de Mello and Raphael B. Kasal  
*Instituto de Física, Universidade Federal Fluminense,  
 Niterói, RJ 24210-340, Brazil*

(Dated: November 11, 2018)

We consider an electronic phase separation process that generates regions of different charge densities, or local dopings, as the origin of the inhomogeneous charge density of high  $T_c$  superconductors. We show that it gives rise to a phase boundary potential between such doping disordered regions or grains. The Bogliubov-deGennes self-consistent calculations in this disordered medium yield position dependent superconducting gaps which are, for all dopings, smaller than those derived from the local density of states with a pseudogap behavior. Studying these two sets of gaps for different temperatures and dopings, we are able to reproduce many many observed properties of superconducting cuprates. This scenario is consistent with a resistivity transition driven by Josephson coupling among the superconducting grains.

PACS numbers: 74.20.-z, 74.25.Dw, 74.62.En, 74.72.Kf

The origin of the superconducting gap associated with the superconducting state and the relation to the pseudogap above the transition temperature ( $T_c$ ) remains one of the central questions in high- $T_c$  research. In this letter, we show that the solution of this important problem is connected to an electronic granular structure derived from an electronic phase separation (EPS) transition.

There are steadily accumulating evidences that the charge distribution is microscopically inhomogeneous in the  $CuO_2$  planes of high temperature superconductors (HTSC)[1–8]. Low temperature Scanning Tunneling Microscopy (STM) has demonstrated non-uniform energy gaps  $\Delta$  that vary on the length scale of nm[2] over the whole surface of these materials. These gaps have two types of shapes[3], and some remain well above the superconducting critical temperature  $T_c(p)$ [4, 5]. More recently, the existence of two types of energy gaps have been observed on electronic Raman scattering experiments[9], STM data[6–8], Angle Resolved Photon Emission (ARPES)[10] and combined STM-ARPES[11]. However, the origin and even the existence of this two-gap picture is still a matter of debate[12, 13].

A possible reason to this complex behavior is an EPS transition driven by the minimization of the free energy[14]. This minimization is due to the formation of anti-ferromagnetic (AF) regions of almost zero local doping ( $p_i \approx 0$ ) with lower free energies than the regions with large local doping level ( $p_i \approx 2p$ ), where  $p$  is the average hole doping of the sample[14]. As  $p$  increases, the Coulomb repulsion in the large local doping regions generates a high energy cost to the phase separation process and the EPS ceases in the overdoped region, in agreement with the disappearance of the local AF fluctuations [15]. This cooperative phenomenon gives rise to (grain) boundary potentials in the  $CuO_2$  planes, single particle bound states and intra-grain superconductivity at low temperature. These superconducting regions develop Josephson couplings among them and the resis-

tivity transition  $T_c(p)$  occurs when the Josephson energy  $E_J(p)$  is equal to  $K_B T_c(p)$ .

We used the theory of Cahn-Hilliard (CH)[16–18] to binary alloys to describe the EPS transition. The transition order parameter is the difference between the local and the average charge density  $u(p, i, T) \equiv (p(i, T) - p)/p$ . In Fig.(1), we show a typical density map with the two (hole-rich and hole-poor) main solutions given by different colors.

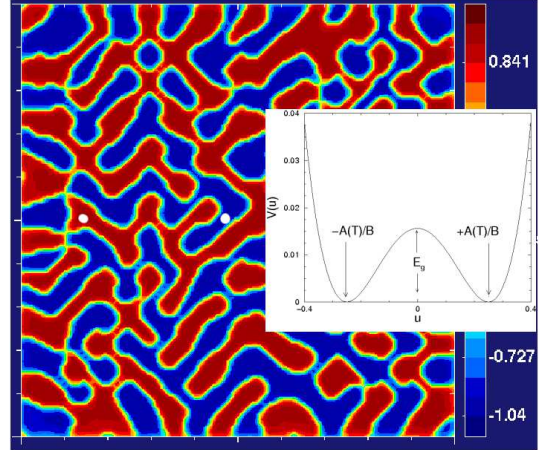


FIG. 1: (color online) The density map simulation of the inhomogeneous charge density on a  $100 \times 100$  sites. In the inset, the GL potential with the two minima representing the two (high and low density) solutions[18] and the potential barrier  $V_{gb}$  between them. Marked white points are located where some calculations shown here were made.

In the inset of Fig.(1) we plot the usual potential from the Ginzburg-Landau (GL) free energy expansion used in the CH equation[14] with its two minima and the potential barrier  $V_{gb} = V_{gb}(p, T)$  between them. The barriers generate shallow potential wells in the  $CuO_2$  planes

that always have an exponential small bound state[19]. These bound states lower the kinetic energy to allow, under favorable conditions, local hole pair formation in the antiadiabatic limit[20].

The calculated  $u(i, T)$  (or  $p(i, T)$ ) density map, as shown in Fig.(1), is used as the *initial input* and it is maintained fixed throughout the self-consistent Bogoliubov-deGennes (BdG) calculations. Notice that the charge inhomogeneity  $p(i, T)$  and  $V_{gb}(p, T)$  are correlated. In what follows, the parameters involved in  $V_{gb}(p, T)$  are chosen to match the average local density of states (LDOS) gaps measured by low temperature STM on  $0.11 \leq p \leq 0.19$  Bi2212 compounds[3]. All others parameters are similar to values previously used[21, 22].

The effect of the temperature in the potential is taken into account using  $V_{gb}(T) \sim (1 - (T/T_{PS})^{1.5})$ , as demonstrated by Cahn and Hilliard[16]. Thus we were able to obtain the intra-grain or *local superconducting temperatures*  $T_c(i)$ , i.e., the onset temperature for the d-wave superconducting gap  $\Delta_d(i, T)$  at a given location  $i$ . The largest value of all  $T_c(i)$  determines the temperature  $T_{on}(p)$  that marks the onset of local superconductivity of the sample.

Similar to granular superconductors[23], the superconducting transition occurs in two steps: first by the appearing of intra-grain superconductivity and then by Josephson coupling with phase locking at a lower temperature. This approach *provides a clear interpretation to the superconducting amplitude and the measured quasi-particles dispersion above  $T_c(p)$* [12, 13].

By using the theory of granular superconductors[24] to these electronic grains and the calculated average superconducting amplitudes  $\Delta_d^{av}(T, p) \equiv \sum_i^N \Delta_d(T, i, p)/N$ , where N is the total number of sites, we can estimate the values of  $T_c(p)$ .

$$E_J(p, T) = \frac{\pi h}{4e^2 R_n} \tanh\left(\frac{\Delta_d^{av}(T, p)}{2K_B T_c}\right). \quad (1)$$

Where  $\Delta_d^{av}(T, p)$  is the average of the local superconducting gaps  $\Delta_d(i, p, T)$  on a  $N \times N$  ( $N = 28, 36$  and  $42$ ) square lattice which are plotted in the top panel of Fig.(2). The inset shows the schematically single particle levels at a shallow puddle whose walls are proportional to  $V_{gb}$ .  $R_n$  is the normal resistance of a given compound, which is proportional to the planar resistivity  $\rho_{ab}$  measurements[25] on the  $La_{2-p}Sr_pCuO_2$  series. In the low panel of Fig.(2), the Josephson coupling  $E_J(p, T)$  is plotted together with the thermal energy  $k_B T$  whose intersection yields the critical temperature  $T_c(p)$ , as shown in the inset. The values are in reasonable agreement with the Bi2212  $T_c(p)$ , as expected, since  $V_{gb}$  was chosen to match the Bi2212 low temperature LDOS[3].

In the BdG approach, the symmetric local density of states (LDOS) is proportional to the spectral function[26]

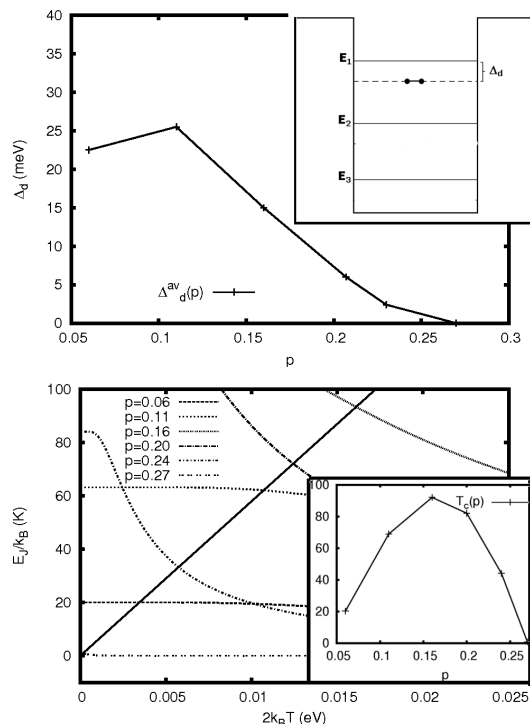


FIG. 2: Top panel, the average  $\Delta_d(p)$ , and in the inset, the schematic single particle and superconducting energy levels in a grain. In the low panel, the thermal energy  $k_B T$  and the Josephson coupling among superconducting grains  $E_J(p, T)$  for some selected doping values as function of T. The intersections give  $T_c(p)$ , as plotted in the inset.

and may be written as

$$N_i(T, V_{gb}, eV) = \sum_n [|u_n(\mathbf{x}_i)|^2 + |v_n(\mathbf{x}_i)|^2] \times [f'_n(eV - E_n) + f'_n(eV + E_n)]. \quad (2)$$

The prime is the derivative with respect to the argument.  $u_n, v_n$  and  $E_n$  are respectively the eigenvectors and eigenvalues of the BdG matrix equation[18, 21],  $f_n$  is the Fermi function and  $V$  is the applied voltage.  $N_i(T, V_{gb}, eV) \equiv LDOS(V_{gb})$  is proportional to the tunneling conductance  $dI/dV$ , and we probe the effects of the inhomogeneous field by examining the ratio  $LDOS(V_{gb} \neq 0)/LDOS(V_{gb} = 0)$ .  $LDOS(V_{gb} = 0)$  contains the inhomogeneous charge distribution and  $LDOS(V_{gb} \neq 0)$  vanishes around the Fermi energy due to the superconducting gap and the single particle levels in the grains. This LDOS ratio yields well-defined peaks and converges to the unity at large bias, in close agreement to similar LDOS ratios calculated from STM measurements[5].

We calculated the LDOS at many values of  $p$  and  $T$  to compare with the STM[2–7] and ARPES[10–13] data, but here we present detailed results only for an under-

doped ( $p = 0.11$ ) and an overdoped ( $p = 0.21$ ) sample. Thus, in Fig.(3) we show the results at two representative places (shown as white dots in the middle of Fig.(1)) of the  $p = 0.11$  sample at various temperatures. In this case, the low temperature LDOS display very few well defined (coherent) peaks but the gaps are similar to the STM data of McElroy et al[3]. The low temperature superconducting gap  $\Delta_d$  produces small anomalies that are marked by arrows, as reported by some STM data[6–8]. This behavior was already noticed by our previous work[14]. Then the gaps derived from the LDOS peaks are identified with the local pseudogap  $\Delta_{PG}(i, p, T)$  because they are larger than the local  $\Delta_d(i, p, T)$  and because they vanish at a higher temperature  $T^*(i)$  than  $T_c(i)$ .

Let us investigate in detail the relationship between  $\Delta_{PG}(i, p, T)$  and  $\Delta_d(i, p, T)$ . For the  $p = 0.11$  compound with  $T_c(0.11) \approx 65\text{K}$  at a typical hole-poor place with  $p_i = 0.02$ , we obtain a low temperature  $\Delta_{PG} \approx 80\text{meV}$  and  $\Delta_d = 12\text{meV}$ . In a representative hole-rich location with  $p(i) \approx 0.23$  there is an interchange of intensity:  $\Delta_{PG} \approx 50\text{meV}$  and the superconducting gap  $\Delta_d(T = 0) = 33\text{meV}$ . We observe that this inversion in the values of  $\Delta_{PG}$  and  $\Delta_d$  is common to all compounds. For this  $p = 0.11$  sample, at all sites,  $\Delta_{PG}(i)$  and  $\Delta_d(i)$  vanish with increasing temperature almost together near  $T = 145\text{K}$ . At the  $p_i = 0.02$  hole poor grain,  $\Delta_{PG}$  and  $\Delta_d$  vanish near  $T^*(i) = T_c(i) = 147\text{K}$ , and at the  $p_i = 0.21$  hole rich grain, they close at  $T^*(i) = 148$  and  $T_c(i) = 146\text{K}$ . We see that, for overdoped samples,  $T^*(i, p) \approx T_c(i, p)$  and they remain much above the resistivity transition  $T_c(0.11) \approx 65\text{K}$ , i.e., *both gaps are present in the pseudogap phase up to  $T^*$* .

The difference between  $T^*(i, p)$  and  $T_c(i, p)$  increases continuously with increasing doping. Calculations with  $p = 0.16$  show that in some grains  $T^*(i) \approx T_c(i) + 15\text{K}$  while in some other locations  $T^*(i) \approx T_c(i)$ . By increasing the doping  $p$ , this difference increases as shown in Fig.(4) for  $p = 0.21$ . For this compound with  $T_c(0.21) \approx 72\text{K}$ , most of the LDOS present well defined coherent peaks as observed by McElroy et al[3]. On the top panel, we show the LDOS at a hole-rich site  $p_i \approx 0.30$ ; we see that  $\Delta_{PG}(T = 40\text{K}) \approx 24\text{meV}$  and  $\Delta_d(T = 40\text{K}) = 7.1\text{meV}$  (marked by arrows in the plots) and they both vanish at  $T^*(i) \approx T_c(i) \approx 72\text{K}$ . At a hole-poor site of  $p_i = 0.9$ ,  $\Delta_{PG}(T = 40\text{K}) \approx 37\text{meV}$  and  $\Delta_d(T = 40\text{K}) = 4.5\text{meV}$ . Following the temperature evolution we see that  $T_c(i) \approx 72\text{K}$  that is also the critical temperature  $T_c(0.21)$ , and  $\Delta_{PG}$  vanishes at much larger value  $T^*(i) \approx 105\text{K}$ . Thus, *the pseudogap phase of overdoped samples is composed mainly by  $\Delta_{PG}$* .

The above results lead us to many conclusions concerning the HTSC measured properties: *i)* The charge inhomogeneities and the charge segregation potential occur due to the formation of (almost zero doping) AF regions. Consequently, its effect is more intense at low doping compounds, leading to large superconducting amplitudes  $\Delta_d$  and  $\Delta_{PG}$  in underdoped samples. On the other

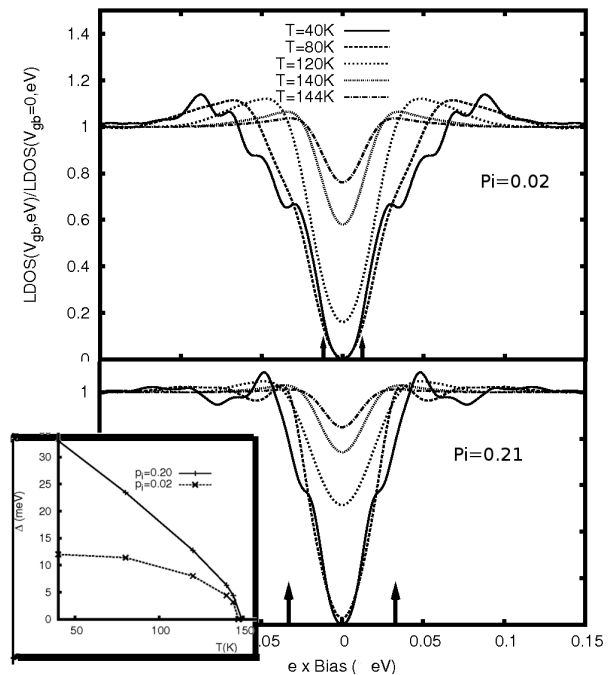


FIG. 3: The  $p = 0.11$  LDOS. Top panel,  $\Delta_{PG}(T)$  at a hole-poor puddle ( $p_i = 0.021$ ).  $\Delta_{PG}(T = 40\text{K}) \approx 80\text{meV}$ . The superconducting gaps  $\Delta_d(T = 40\text{K}) = 12\text{meV}$  are marked by arrows. Below, the set of LDOS curves at a hole-rich grain, ( $p(i) \approx 0.20$ ) with  $\Delta_{PG}(T = 40\text{K}) \approx 50\text{meV}$  and with  $\Delta_d(T = 0) = 33\text{meV}$ . In the inset  $\Delta_d(i, T) \times T$  for each case. Both  $\Delta_{PG}(i)$  and  $\Delta_d(i)$  vanish near  $T = 147\text{K}$ .

hand, at far overdoped region, the large Coulomb repulsion in the hole-rich grains destroys the EPS transition and the superconductivity. *ii)* As in granular superconductors, the resistivity transition occurs by Josephson coupling among the intragrain superconducting regions. *iii)* In this scenario, the pseudogap is due to the weakly localized energy levels in the two dimensional puddles and it is not directly related to the intragrain superconductivity, although both phenomena are originated by the segregation potential  $V_{gb}$ . This different process was demonstrated by the distinct behavior of the two signal with applied magnetic fields and also with the temperature in tunneling experiments[27]. *iv)* The observed difference in the LDOS form, called "coherent" and "zero temperature pseudogap"[3], is due to the LDOS at hole-rich and hole-poor locations respectively. This distinction is clearly seen in the overdoped calculations (Fig.(4)) where most LDOS presents coherent peaks in opposition to the underdoped case (as in Fig.(3)) where the rounded and ill-defined peaks are more abundant. *v)* The hole-poor regions have basically one electron per unit cell and the large Coulomb repulsion generates a large asymmetry between electron extraction and injection as measured by the STM experiments[2–8]. The

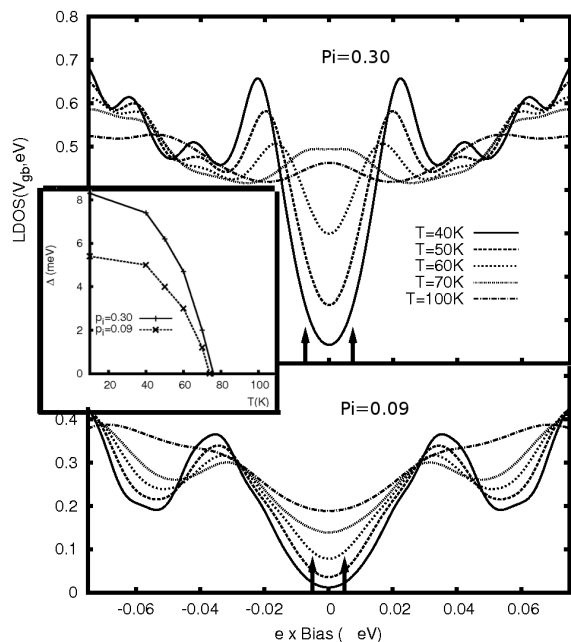


FIG. 4: LDOS for overdoped  $p = 0.21$ . At the top,  $\Delta_{PG}(T)$  at a hole-rich grain ( $p_i \approx 0.30$ ) yielding  $\Delta_{PG}(T = 40K) \approx 24\text{meV}$  and  $\Delta_d(T = 40K) = 7\text{meV}$  marked by the arrows. Below,  $\Delta_{PG}(T)$  at an "insulator" grain ( $p(i) \approx 0.09$ ),  $\Delta_{PG}(40K) \approx 37\text{meV}$  and  $\Delta_d(T = 40K) = 4.5\text{meV}$ . In the inset, we show also that  $\Delta_d(T) \times T$  at the two locations. It is important to notice that  $\Delta_{PG}(i)$  remains even above  $T = 100\text{K} \gg T_c(i)$  for some hole-poor grains  $i$ .

LDOS at hole-rich regions, like a homogeneous system, are expected to be more symmetric. *vi*) The observed anomaly or kink measured in the LDOS at very low bias[6–8] was demonstrated to be due to the low temperature superconducting gap  $\Delta_d$ . Fig.(3) shows clearly a small kink marked by the arrows. In general, it is more visible in underdoped samples because the  $\Delta_{PG}$  is

much larger than  $\Delta_d$ . *vii*) For underdoped samples, as in Fig.(3),  $\Delta_d$  and  $\Delta_{PG}$  remain finite much above and vary very little around  $T_c(p) \approx 65\text{K}$ . The presence of the superconducting gap and its quasiparticle dispersion above  $T_c(p)$  was measured in weakly underdoped Bi2212 by ARPES experiments[12] that also showed that the gap ( $\Delta_{PG}$ ) almost does not change around  $T_c(p)$ . *viii*) The ARPES experiment of Lee et al[10] has measured increasing gapless Fermi arcs along the nodal  $(\pi, \pi)$  region with increasing doping above  $T_c(p)$ . As we have shown, the d-wave  $\Delta_d$  remains above  $T_c(p)$  in the underdoped regions but tends to vanish close to  $T_c(p)$  for overdoped compounds. Assuming that the weakly bound states ( $\Delta_{PG}$ ) are due to the random phase boundary potential  $V_{gb}$ , and that they occur mainly along the  $Cu-O$  (antinode) direction, together with the d-wave behavior of  $\Delta_d$  is agreement with the increase of the gapless Fermi arcs with  $p$  above  $T_c(p)$ [10]. *ix*) The calculations show that, in general, for any compound, the pseudogap  $\Delta_{PG}$  is smaller but with well defined peaks at the hole-rich regions than in the hole-poor ones. Consequently, the measured larger  $\Delta_{PG}(i)$  gap values located at the low density grains with local (AF) insulator behavior have lower local conductivity ( $dI/dV$ ) than the smaller gaps (and higher densities) as verified by Pasupathy et al[5]. *x*) The STM measured relation  $2\Delta/K_B T^*(i) \approx 8.0$ [4] is reproduced closely by the optimal and the  $p = 0.21$  sample, considering  $\Delta = \Delta_{PG}(i)$  and its associated  $T^*(i)$ .

In summary, we have proposed an EPS transition to describe the inhomogeneous charge distribution of HTSC generated by the lower free energy of the (undoped) AF domains. This approach yields potential wells with shallow bound states that reduce the kinetic energy and favor the superconducting pairing. The calculations obtain the inverted bell shape critical line  $T_c(p) \times p$ , distinguish clearly the LDOS pseudogap  $\Delta_{PG}$  from the intragrain superconducting gap energy  $\Delta_d$  and provide simple physical interpretations to many different STM and ARPES results.

We gratefully acknowledge partial financial aid from Brazilian agency CNPq.

- 
- [1] J.M.Tranquada, et al Nature (London),**375**, 561 (1995).  
[2] S. H. Pan et al, Nature (London), 413, 282-285 (2001).  
[3] K. McElroy, et al cond-mat/0404005 an Phys. Rev. Lett. **94**, 197005 (2005).  
[4] Kenjiro K. Gomes et al, Nature **447**, 569 (2007).  
[5] Abhay N. Pasupathy et al, Science **320**, 196 (2008).  
[6] Takuya Kato et al, J. Phys. Soc. Jpn., **77**, 054710 (2008).  
[7] Aakash Pushp et al, Science **324** 1689 (2009).  
[8] T. Kato et al, J. Supercond. Nov. Magn. **23**, 771 (2010).  
[9] M. Le Tacon, et al, Nature Phys. **2**, 537 (2006).  
[10] W. S. Lee, et al, Nature **450**, 81 (2007)  
[11] J. H. Ma, et al, Phys. Rev. Lett. **101**, 207002 (2008).  
[12] A.Kanigel et al, Phys. Rev. Lett. **101**, 137002 (2008).  
[13] U. Chatterjee, et al Nature Phys. **6**, 99 (2010).  
[14] E.V.L. de Mello, et al J. Phys.: Condens. Matter **21**, 235701 (2009).  
[15] S. Wakimoto et al Phys. Rev. Lett. **98**, 247003 (2007)  
[16] J.W. Cahn and J.E. Hilliard, J. Chem. Phys, **28**, 258 (1958).  
[17] E.V.L de Mello et al, Physica **A 347**, 429 (2005).  
[18] E.V.L. de Mello et al, Phys. Rev. **B70**, 224517 (2004).  
[19] L.D. Landau, and E.M. Lifshitz, "Quantum Mechanics", Pergamon Press, New York, 1977.  
[20] E. V. L. de Mello, et al, Phys. Rev. **B58**, 9098 (1998).  
[21] D. N. Dias et al, Phys. **C468**, 480 (2008).  
[22] E.V.L. de Mello et al, Physica **B404**, 3119 (2009).  
[23] L. Merchant et al, Phys. Rev. **B63**, 134508 (2001).  
[24] V. Ambeogakar, and A. Baratoff, Phys. Rev. Lett. **10**,

486 (1963).

[25] H. Takagi et al, Phys. Rev. Lett. **69**, 2975 (1992).

[26] François Gygi, and Michael Schlüter, Phys. Rev. **B43**,

7609 (1991).

[27] V. M. Krasnov et al, Phys. Rev. Lett. **86**, 2657 (2001).